



## **PART I**

# Instrumentation, Imaging Techniques, and Protocols

COPYRIGHTED MATERIAL

P1: SFK/UKS P2: SFK Color: 4C  
c01 BLBK309-Dilsizian June 9, 2010 17:20 Trim: 254mm X 178mm Printer Name: Yet to Come

# 1

## CHAPTER 1

# Positron Emission Tomography

*Stephen L. Bacharach*

University of California, San Francisco, CA, USA

The goal of all cardiac nuclear imaging is to trace the fate of radioactively labeled biochemical compounds (tracers) within the body, usually in the myocardium or blood pool. One usually either makes a static image of the distribution of the radiotracer (e.g.,  $^{18}\text{F}$ -fluorodeoxyglucose ( $^{18}\text{FDG}$ ) or thallium-201 ( $^{201}\text{Tl}$ )) or follows the uptake and clearance of the tracer with time. In the former case, static imaging is all that is required, while in the latter a series of images, acquired dynamically over time, is necessary. Positron emission tomography (PET) has these same goals. Although PET works in a manner very similar to conventional tomographic nuclear imaging techniques (e.g., single photon emission computed tomography or SPECT), there are some very significant differences. It is these differences that make PET of great potential value in nuclear cardiology, and it is these differences we will emphasize in this chapter.

### Positron Decay

PET tracers, as their name implies, decay by emission of a positron. Except for their opposite charge, positrons are nearly identical to ordinary negatively charged electrons (which in fact are often called “negatrons”). They have the same mass and behave similarly when passing through the body. Positrons, however, are the “antimatter” of electrons. When a positron and an electron are in close proximity for more than the briefest interval, both will disappear (called “annihilation”), and their masses will be converted into energy

in the form of two gamma rays traveling in almost exactly opposite directions. The energy of each photon is 0.511 meV (exactly the equivalent energy corresponding to the mass of the electron or positron). These photons are sometimes called “annihilation” photons. The two photons travel in nearly exactly opposite directions in order to conserve momentum. The entire process is illustrated in Figure 1.1. In this figure it is assumed that a positron emitter (in this case carbon-11 ( $^{11}\text{C}$ )) is emitted by a tracer somewhere in the body (e.g., the myocardium). When the positron is emitted from the nucleus it is traveling at very high speed—nearly the speed of light. It moves through the tissue just as an electron would, bouncing off many of the atoms and losing energy as it does so. Eventually (typically within a millimeter or so, depending on the radionuclide) it slows down enough to spend a significant time near an electron. As soon as this happens the two annihilate and the two gamma rays (each with 0.511 meV) are emitted, as shown in Figure 1.1, each going in nearly the exact opposite direction. Although in Figure 1.1 the annihilation photons are shown traveling in exactly opposite directions, occasionally photons are emitted a few tenths of a degree more or less than  $180^\circ$  apart.

PET scanners detect pairs of gamma rays resulting from annihilation. By determining where these two gamma rays (and all other pairs of gamma rays) originated, the PET scanner can produce an image showing the location in the body where the positrons have annihilated. However, if the positron has traveled far from its parent atom, the image will be inaccurate—the locus of the annihilating positron will not correspond to the locus of the radioactive atom. For this reason the initial speed

4 PART I Instrumentation, Imaging Techniques, and Protocols

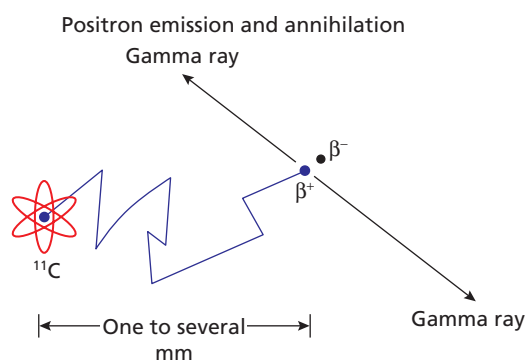


**Figure 1.1** A positron is shown being emitted from the nucleus of  $^{11}\text{C}$ . It is assumed that the  $^{11}\text{C}$  atom is located in tissue. The positron is initially emitted at a speed which is a significant fraction of the speed of light. As it passes through the tissue, it gradually slows down, as it bounces off the atoms in the tissue. Eventually it slows down sufficiently so that it spends significant time near an atomic electron—its antimatter equivalent. When this happens the electron and the positron both annihilate—their mass being converted to energy in the form of two photons traveling in opposite directions, as shown.

(i.e., energy) of an emitted positron will affect the capacity of the PET scanner to accurately define the position of radioactive atoms within the myocardium. This in turn affects the ultimate spatial resolution of the images that can be obtained with a PET scanner.

There are many radioisotopes that emit positrons, and so would be suitable for use with a PET scanner. Several of the most important ones are listed in Table 1.1, along with their half-lives and some characteristics of the positron that is emitted

[1]. One of the reasons why PET has played such an important role in basic research is that several of the radioisotopes that are positron emitters (carbon, nitrogen, and oxygen) are the basic building blocks of all physiologically important biochemical compounds. This has permitted researchers to label amino acids, glucose, and a host of other biochemical compounds. Unlike the case with technetium-99m ( $^{99\text{m}}\text{Tc}$ ), the labeling can often be done without making any alterations to the biochemical structure of the compound of interest. That is, a nonradioactive  $^{12}\text{C}$  atom can be replaced with a  $^{11}\text{C}$  atom, so that the resultant radiolabeled biochemical compound behaves just like the unlabeled one. The difficulty with  $^{11}\text{C}$ , nitrogen-13 ( $^{13}\text{N}$ ) and oxygen-15 ( $^{15}\text{O}$ ) is that their half-lives are very short. This means they must be produced locally with an on-site cyclotron. It also means that the chemist in charge of labeling the biochemical compound of interest has very little time to do so. For these reasons (and others discussed below), the two most clinically important positron-emitting isotopes for cardiology are the last two on the list, fluorine-18 ( $^{18}\text{F}$ ) and Rubidium-82 ( $^{82}\text{Rb}$ ).

$^{18}\text{F}$  has a 2-hour half-life. This is long enough to allow production at a site up to a few 100 km away. The recent dramatic increase in the use of  $^{18}\text{F}$ FDG for tumor imaging has resulted in a large number of such commercial production sites in the US (and to a lesser extent abroad). One can easily arrange for delivery of daily unit doses of  $^{18}\text{F}$ FDG.  $^{18}\text{F}$ FDG has proven very valuable in assessing myocardial viability [2]. Its use for this purpose has, in the past, been limited to large research institutions because

**Table 1.1** Positron energies and ranges (in tissue).

Isotope	Maximum energy (meV)	Average energy (meV)	Average distance positrons travel (mm)	Maximum distance positrons travel (mm)
$^{18}\text{F}$	0.635	0.250	0.35	2.3
$^{11}\text{C}$	0.96	0.386	0.56	4.1
$^{13}\text{N}$	1.19	0.492	0.72	5.2
$^{15}\text{O}$	1.72	0.735	1.1	8.1
$^{88}\text{Ga}$	1.90	0.836	1.1	9.4
$^{82}\text{Rb}^{\text{a}}$	3.35 (83%)	1.52	2.4	16.7

<sup>a</sup>Rb emits two different positrons. Eighty-three percent of the time it emits a 3.35-meV maximum energy positron and 12% of the time a 2.57-meV positron.

of the lack of availability of  $^{18}\text{F}$ FDG and a PET scanner. As mentioned,  $^{18}\text{F}$ FDG is now widely available commercially, and there are a huge number of new PET scanners which have been installed, the majority in nonresearch hospitals. Although most of these scanners were installed for oncology imaging, the machines are often suitable for cardiac imaging as well.

The other clinically important radiopharmaceutical in Table 1.1 is  $^{82}\text{Rb}$ . This is a potassium analog and can be used to measure myocardial perfusion [3]. No labeling is required. Although it has a very short half-life (76 seconds), it can be produced from a longer lived  $^{82}\text{Sr}$  generator, with a half-life of 25 days. At the moment such generators are fairly expensive, but the cost is expected to drop substantially if demand increases.

Aside from half-life, two other factors must be considered when determining the utility of a positron-emitting isotope. First, it is important that nearly all the decays are by positron emission, rather than by other forms of decay whose emissions cannot be imaged with a PET scanner.  $^{11}\text{C}$ ,  $^{13}\text{N}$ , and  $^{15}\text{O}$  all decay nearly 100% of the time by positron emission, and  $^{82}\text{Rb}$  decays about 95% of the time by positron emission [4]. The remaining fraction of the decays is by electron capture—a process that produces radiation that cannot be imaged with a PET scanner. In addition, for  $^{82}\text{Rb}$  a small fraction (~12%) of the positrons are accompanied by an additional high-energy gamma ray (0.778 MeV) which can produce some interference with imaging the 0.511-MeV annihilation photons and which increases radiation exposure slightly. There are other positron emitters (e.g.,  $^{94}\text{Tc}$ ,  $^{124}\text{I}$ , several isotopes of Cu, and many others) that have an even larger number of other emissions and other significant modes of decay. This often results in poorer dosimetry for the patient because these emissions may increase the patient's radiation exposure, but do not produce useful imaging information. Nonetheless, many of these isotopes have been used successfully in PET imaging.

The second factor one must consider when evaluating a radioisotope is the energy of the positron that is emitted. As mentioned above, this is important because what one images with a PET scanner is not the distribution of the radiotracer, but rather the distribution of the annihilation photons.

Positrons are not emitted with a single characteristic energy as are gamma rays. Instead they have a range of possible energies from 0 up to a characteristic maximum energy. Each positron-emitting radionuclide has its own characteristic maximum and average energy of positron emission, as shown in Table 1.1. Because of this, and because the path of the positron as it slows down is quite tortuous (e.g., Figure 1.1), not all the positrons emitted by a given type of atom travel the same distance—some travel quite far and others do not. Table 1.1 also shows the average distance from the parent atom each positron travels in tissue. The positrons emitted by  $^{18}\text{F}$  have a very low energy. Thus, on average they travel only a very small distance away from the parent atom (about 0.35 mm). In contrast,  $^{15}\text{O}$  emits positrons that are considerably more energetic and travel an average of 1.1 mm. Positrons from  $^{82}\text{Rb}$  travel an average of 2.4 mm. Because the spatial resolution in a cardiac PET image can be as good as ~5–7 mm, the extra blurring caused by the range of travel in tissue can be significant for isotopes such as  $^{82}\text{Rb}$ , and to a lesser extent,  $^{15}\text{O}$ .

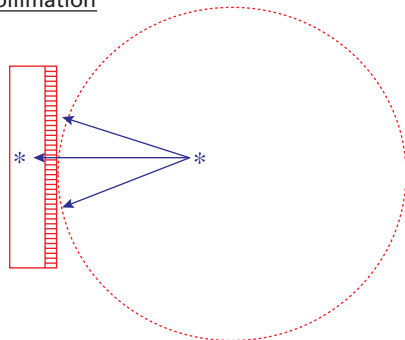
Before we can further discuss the characteristics of PET scanners, it is necessary to understand how tomographic images are made and how they are “reconstructed” from the radioactivity seen by the ring of detectors surrounding the patient. Many treatises have been written dealing with the mathematical steps necessary to produce cross-sectional images with emission tomographs [5]. Here we will describe the reconstruction process in a physical, rather than in a mathematical, way.

To define the three-dimensional (3D) shape of an object, one must first be able to look at the object from all sides. This may be an evolutionary advantage of binocular vision (two eyes, not one). Each eye's slightly different view of the same object, when processed by the brain, allows formation of a 3D image of the object's surface. Because our eyes are not placed very far apart we cannot see all sides of an object at once, and so we must extrapolate (often incorrectly) using the information from the two angles we can see in order to visualize the object's full appearance. In a similar manner, a physician may wish to examine several planar  $^{201}\text{Tl}$  scans, each taken at a different angle, in an effort to mentally reconstruct the 3D distribution of  $^{201}\text{Tl}$  in

6 PART I Instrumentation, Imaging Techniques, and Protocols

Need to know Where photons came from

Extrinsic collimation



Collimator tells us where gamma ray came from

**Problem:** Collimators block about 999/1000 photons. *Very low sensitivity device.*

**Figure 1.2** In single photon tomography (SPECT) a collimator is needed to tell the direction from which the gamma ray came. The camera must then rotate around the patient (the dashed line shows the rotation) in order to measure the projection images at every angle.

the myocardium. The situation in this case is more complex because nuclear medicine images portray not just the surface of an object, but its interior as well. That is, the object is transparent (except for attenuation) to its radiation.

Just as all sides of an object must be seen by the eye and brain to appreciate its 3D surface, many two-dimensional (2D) planar views, each taken at a different angle, are necessary to allow determination of the 3D interior activity concentration of an object. Each of these 2D views at a particular angle is referred to as a “projection.” The reconstruction process (i.e., the method for producing tomographic slices) is based on acquiring these projections. PET, SPECT, and even computed tomography (CT) must all acquire projection images, and in fact all use a similar method for reconstructing the 2D projection images into tomographic slices. The only difference is in how each modality obtains its projection images. In SPECT these “projection” images are obtained by rotating a gamma camera around the object being imaged, as in Figure 1.2. In CT the views are obtained by rotating an X-ray tube around the patient and measuring how many photons are able to get through the body (so each projection is just a planar X-ray image—see Figure 1.3). We will see shortly how PET accomplishes the same thing—creating a planar image of the positron annihilation radiation at each angle.

In theory, an infinite number of projections are necessary to define the 3D distribution of activity in an object. In practice, cardiac SPECT images are

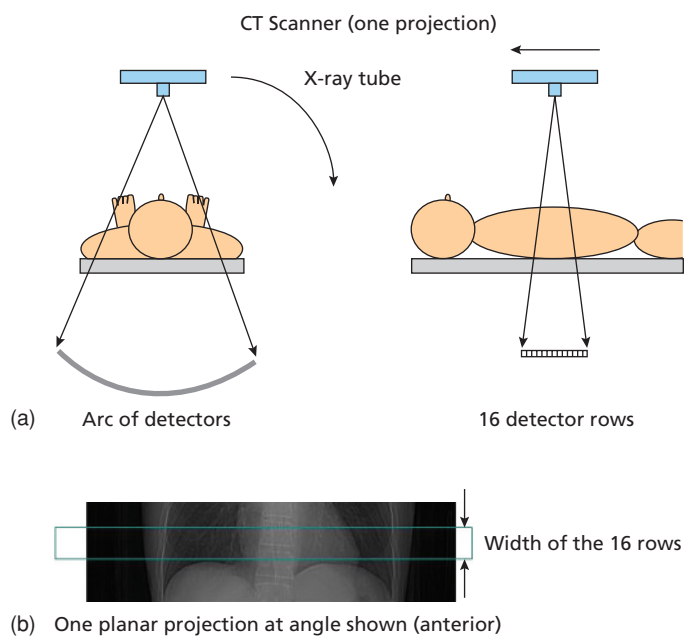


**Figure 1.3** In X-ray computed tomography (CT) the X-ray tube must move around the body (a) to acquire projection images just as the gamma camera must move around the body in SPECT. Image (b) shows one planar projection. The tomographic image can be reconstructed from a set of these projections at all angles.

usually reconstructed from fewer than 100 angles, while several hundred different views, each at a different angle, are usually acquired for PET.

Once the PET (or SPECT or CT) scanner has collected data from all these projections, or views, several steps are necessary to create a tomographic slice. The details of these steps [5] are unimportant for understanding the rest of this chapter. They may be considered simply as mathematical operations that convert the many projection images into a single tomographic section or slice.

PET scanners can simultaneously obtain all the views necessary to reconstruct a tomographic image with the use of a ring (or multiple rings) containing hundreds or thousands of detectors that encircle the patient. The mechanical assembly holding all these detectors is called the “gantry.” The means by which the ring of detectors acquires data for the many views required can be explained by first remembering the basic information that is needed to perform the reconstruction, i.e., the projection images. A projection image is made up of all the photons that came from a certain direction (projection angle). In the SPECT example of Figure 1.2 the camera is able to show from which direction the photons have come by using a collimator [6]. All photons that do not strike the camera perpendicular to its face are blocked by the collimator. So in Figure 1.2 the number of gamma rays detected at each point on the gamma-camera face must have come only from  $270^\circ$  (numbering angles clockwise, with 0 at the top). Unfortunately, blocking all the photons arriving from other angles is a very inefficient way to make a projection image. Many collimators block more than 999 out of every 1000 photons emitted by the radioactive atoms in the patient. Such a SPECT device would therefore waste over 99.9% of all the photons emitted by the patient. That is the price one pays for using a collimator to determine what direction the photons came from. PET can get the same information—how many photons were emitted and what direction they came from—without a collimator, potentially making PET far more sensitive than SPECT. How is this done? Consider Figure 1.4a, showing a ring of detectors surrounding the patient. Only four of the hundreds of detectors are shown (and those four are shown greatly enlarged for clarity). Imagine that a 511-keV photon has just struck detector 3, as in Figure 1.4a. If this were the

only piece of information that the PET scanner had, it would not be of any use. We would know that an annihilation had occurred, but we would not know from which direction it had come. It could have come from almost any direction. However, recall that for annihilation photons, there is always another photon traveling in the opposite direction. Therefore, if a 511-keV photon struck detector 3 and simultaneously (i.e., in “coincidence”) another 511-keV photon struck detector 2, then the computer would realize that this pair of photons must come from a positron that annihilated somewhere along the line B connecting the two detectors (see Figure 1.4a). This is useful information—we know an annihilation occurred and we know from which direction the two photons came. This method of determining where the photons came from, without a collimator, is called “coincidence imaging” [7]. In reality the two photons may not be detected truly simultaneously. For example, the annihilation may occur closer to one of the detectors than the other, and so may reach that detector first (although the difference in time is usually on the order of a billionth of a second). One therefore usually accepts any pair of photons that occur within a narrow time interval as being in “coincidence.” This window is called the “coincidence window” or “timing window” or the “resolving time” of the scanner, usually designated by the symbol  $\tau$ . It is typically 5–20 ns wide, depending on the scanner.

The pairs of detectors in Figure 1.4b connected by solid lines (A-1, B-2, etc.) provide one “view” of the object at a given angle. Coincidences between A-2, B-3, C-4, etc. (dashed lines on Figure 1.4b) provide another view of the object, at a slightly different angle. The PET camera has electronic circuits that can distinguish coincidences from every possible pair of detectors in the field of view of the camera.

In Figure 1.4b, the solid lines comprising one “view” or projection are spaced rather far apart. To allow the PET scanner to distinguish small objects from one another, it is desirable that these lines be as close together as possible. This is accomplished by making the width of each detector small and placing the detectors as close together as possible. This decreases the spacing between lines and increases the number of possible angles (and therefore the number of views). Of course, increasing the total number of possible coincidences in this

8 PART I Instrumentation, Imaging Techniques, and Protocols

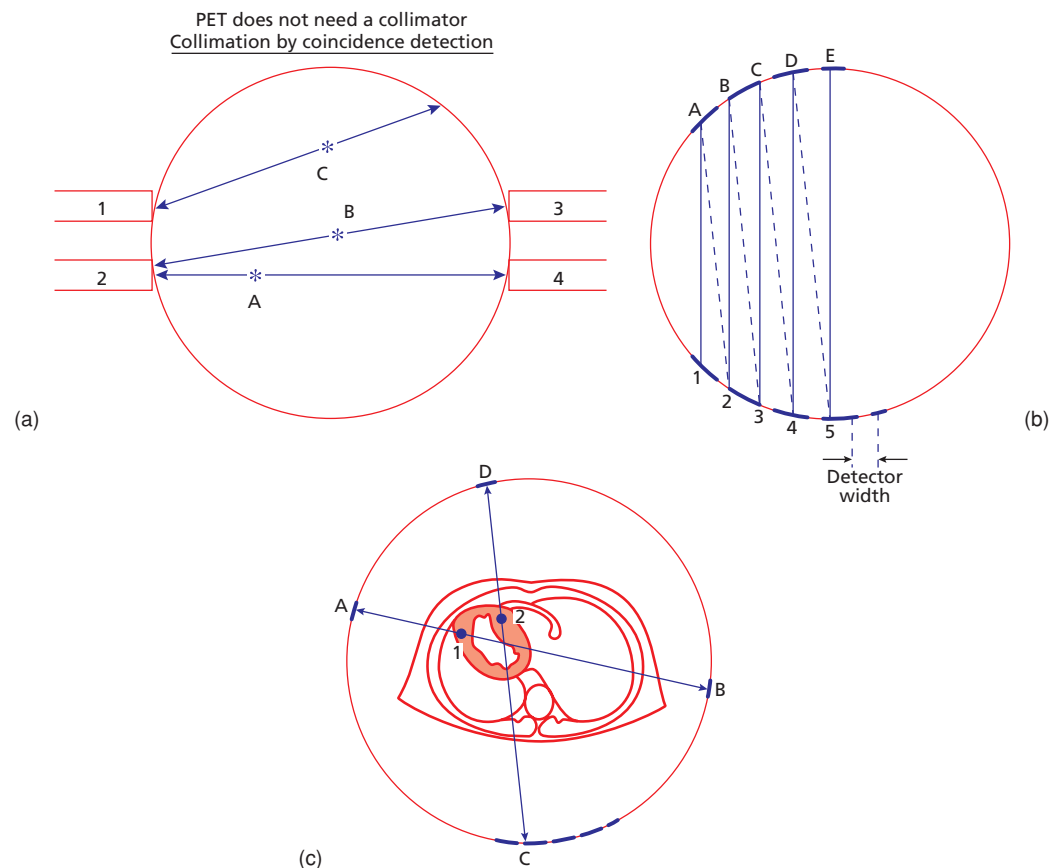


**Figure 1.4** (a) Showing how the direction from which a photon came can be determined in positron emission tomography (PET) by use of coincidence detection. When detectors 2 and 3 both detect a photon at the same time, the computer deduces that the pair of photons must have come from an annihilation along the line connecting detectors 2 and 3, as shown. (b) Showing how groups of

detector pairs can form a projection image at a particular angle. Two projection angles are shown—the solid line shows the anterior–posterior projection, while the dashed lines show a projection about 10° shifted. (c) Showing a schematic diagram of coincidence detection among the crystals of one ring of detectors.

way increases the number of crystals, coincidence circuits, and other electronic components required, making the PET scanner more costly.

A factor that limits the number of crystals employed in a PET scanner is the number of photomultiplier tubes required. When a detector “detects” a gamma ray, it produces a small flash of light that is converted to an electronic pulse by a photomultiplier tube. Ideally each crystal would be attached to one photomultiplier tube, but the tubes cannot be made arbitrarily small and are quite expensive. Thus, manufacturers have devised schemes to allow one photomultiplier tube to share many crystals. A schematic diagram of coincidence detection among

the crystals of one ring of detectors is shown in Figure 1.4c.

Most scanners for cardiac imaging use several rings of detectors, often separated by high atomic number shielding (e.g., lead, tungsten) called “septa,” to acquire data for multiple slices. When a PET scanner is operated with septa between rings it is said to be operating in “2D” mode. This is a bit of a misnomer, since of course such a scanner still acquires 3D data. As will be discussed later, some scanners operate without the septa. Those scanners are said to be operating in “3D” mode [8–11]. To increase the number of slices, coincidences are often recorded between one detector in

one ring, and an opposing detector in an adjacent ring. Such a slice would be called a “cross” slice. With three rings of detectors (numbered I, II, and III) five slices could be produced. The first would consist of all coincident events from opposing pairs of detectors in ring I (a direct slice); the second would be a cross slice consisting of all coincident events between one detector in ring I and an opposing detector in ring II (or vice versa); the third would be formed from events only in ring II, and so on. Some PET scanners have completely separate rings of detectors. With this design, what constitutes a cross slice and what constitutes a direct slice is obvious. Other scanners have crystals so close together in the  $Z$ -axis that the concept of physically separate rings no longer applies. What is important in any case is the final spatial resolution obtained (in all three directions) and the number of, and spacing between, slices.

Cardiac PET scanners reconstruct transaxial slices. The number and spacing of the slices is usually such that at least a 15-cm axial distance is encompassed by the slices—a quite adequate size for cardiac imaging—large enough to include the entire left ventricle in nearly all subjects. Depending on the scanner anywhere between 30 and 70 slices or more cover this  $\sim 15$ -cm axial field of view. It is often desirable to include some of the left atrium in the image also (even though it is not usually visualized well) to allow arterial blood concentrations of tracer to be measured. Some scanners permit a slight rotation and tilt of the gantry, but no scanner presently available can be positioned to yield true cardiac short-axis slices directly. Rather, one reformats the transaxial slices into short- or long-axis views.

It is important to understand the quantity being measured in the reconstructed image obtained from a PET scan. Each of the projections described previously measures simply the total number of coincidences seen by each detector pair at a given angle during a specific time period (the scan time). For example, in Figure 1.4b, one projection is formed by the solid lines A-1, B-2, etc. The quantity measured by each detector pair in this projection is the number of coincidences/second seen along the line, for example that formed by A-1. This “line” is not an infinitesimally thin line, but has a width, because the detector pair A and 1 both have fi-

nite width. The number of coincidences seen by the pair A and 1 are those produced by all the radioactive material lying in the volume between them. The units of the measurement are therefore “coincidences/second/volume.” These projection data are reconstructed to determine the number of coincidences arising from each point in the final reconstructed image. Since each point in the image also represents a small volume in the object being imaged, the units are again coincidences/s/volume. Finally, it is assumed that the number of coincidences/second measured in a volume is directly proportional to the amount of radioactive material (usually measured in Bq (Bequerels) or Ci (Curies)) in that same volume. Providing all the corrections described below are made, this assumption is correct. The units of the PET scan can therefore be any of the following: coincidences/s/cc, Bq (or nCi)/cc, or grams of radiolabeled material/cc. Use of the last unit is possible because Bq can be easily converted to number of atoms or grams as long as the half-life is known.

### Accidental Coincidences

Unfortunately, it is possible for two photons that did not come from the same annihilation event to be erroneously identified, quite by accident, as having occurred “simultaneously,” that is, within the resolving time  $\tau$  of the PET scanner.

Figure 1.5 illustrates such a case. Only one of the photons from annihilation A has reached a detector; the other missed the ring. At nearly the same time atom B decayed. Only one of its photons was detected, the other also missing the ring. If these two separate events happen to occur at nearly the same time within the resolving time of the PET scanner, they will be considered to be in coincidence. The PET scanner then will falsely treat the detection of the two photons as if they resulted from a single annihilation that took place along the line between the two detectors (the dashed line in Figure 1.5). Such false coincidence is called an accidental or random coincidence. Random coincidences produce background activity in the reconstructed image that varies slowly in magnitude at different positions over the image, depending on the radioisotope distribution.

10 PART I Instrumentation, Imaging Techniques, and Protocols

- Randoms
- Two single, unrelated photons are accidentally detected at same time
  - # Randoms  $\propto$  (activity)<sup>2</sup>

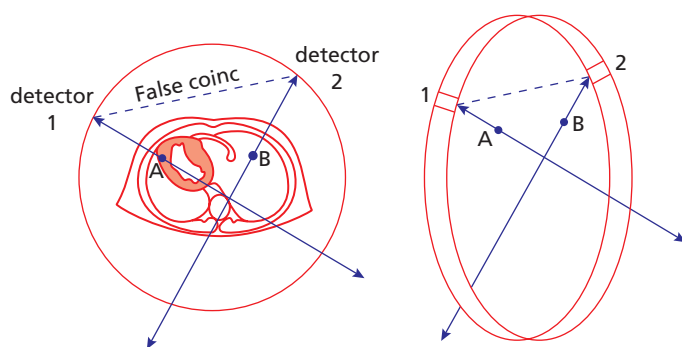


**Figure 1.5** Illustrating how if by accident, two separate annihilation events (A and B) are detected at nearly the same time a false or “accidental” coincidence can occur. This accidental (or “random”) coincidence causes the PET camera to erroneously think the annihilation occurred along the dashed line indicated.

Accidental coincidences between unrelated photons must be distinguished from “true” coincidences between pairs of annihilation photons. The probability that an accidental coincidence will occur depends on the duration of the resolving time interval,  $\tau$ : if it is very long, it becomes much more likely for two unrelated photons to be accidentally in coincidence. The resolving time of a PET scanner is therefore an important parameter, defining how well the scanner will distinguish true coincidences from accidental ones.

A second factor influencing the number of accidental events recorded is the amount and location of activity detected by the PET scanner. If the activity within the patient is doubled, the number of true coincidences will of course double also. The number of accidental coincidences, however, will increase by a factor of 4, i.e., as the square of activity. This has important ramifications. At sufficiently high levels of activity (e.g., for <sup>82</sup>Rb scans [9,11,12]), the number of accidental coincidences may equal or even exceed true coincidences. With administration of excessive amounts of tracer, the patient may, therefore, be exposed to a higher radiation risk without a comparable increase in the amount of useful information obtained. The amount of activity constituting an excess varies with the machine used; it may be only a few millicuries in the field of view or as much as 50 or more mCi. Many manufacturers specify the concentration of activity that when placed in a specified phantom will produce equal numbers of true and accidental coincidences. This

is useful to help evaluate the maximum activity that one might inject in a patient from the point of view of excessive randoms.

The reason that accidental events increase as the square of activity can be discerned from consideration of Figure 1.5. Suppose that detector one measures  $S_1$  ( $S$  refers to “singles”) counts/second, independent of whether these counts were in coincidence with any other detector. The count rate observed by a single detector, as opposed to a coincident pair of detectors, is called the singles count rate of that detector. Suppose also that detector 2 measures a singles rate of  $S_2$ /second. Consider that one photon has just struck detector 1. If an unrelated photon were to hit detector 2 within the next  $\tau$  seconds or has already hit detector 2 within the previous  $\tau$  seconds, it will be in accidental coincidence with the event recognized by detector 1. Because there are  $S_2$  events detected by detector 2 each second, the number of these that will occur during the  $\tau$  seconds before or the  $\tau$  seconds after the event in  $S_1$  is  $S_2 \times 2 \times \tau$ . For every photon that strikes detector 1, there are therefore  $2 \times \tau \times S_2$  accidental coincidences/second. However, there are  $S_1$  photons striking detector 1 every second. Therefore the total number of accidental coincidences/second is:

$$\text{Accidental coincidences/second} = 2 \times \tau \times S_1 \times S_2$$

If the activity in the patient is doubled, the singles rate for every detector is also doubled, so both  $S_1$  and  $S_2$  double, giving a factor of 4 increase in accidental coincidences.

Consideration of the above equation suggests a way to correct for accidental coincidences. If the singles rate is measured at every detector, the number of accidental coincidences can be computed for every detector pair, and this number can be subtracted from the measured true events. Although measured singles rates include some counts from true coincidences, singles rates usually greatly exceed true coincidence rates. Thus, the error introduced by such a correction scheme is usually quite small.

Another approach to correction for random coincidences is the delayed coincidence method. Consider a single pair of opposing detectors in Figure 1.4. The output of detectors is split. One of the signals goes to the coincidence circuitry as usual. The other goes to a special circuit (or even a long length of wire) that causes a prolongation of travel time for the signal, perhaps of several 100 ns. This second wire is connected to the usual circuit, which determines whether the two pulses (one from the delayed signal from the second wire of one detector, and the second from the undelayed, first wire of the opposing detector) occurred within time  $\tau$  of each other. If a true coincidence event occurs, the delayed signal traveling down the second wire will not register as a coincidence with the undelayed signal of the opposing detector. The signal traveling down the long wire would reach the coincidence electronics much later than the undelayed signal from the opposing detector. Any coincidences measured by this long wire would, therefore, only be accidental coincidences and not true coincidences. They could, therefore, be subtracted from the total number of coincidences measured with the undelayed standard short wires of both detectors to yield the number of true coincidences. The delayed coincidence method is quite accurate. However, it is limited by low signal-to-noise ratios because the number of randoms measured by the second delayed wire is often quite small, which may introduce additional noise into the final corrected image. On the other hand, use of the singles method discussed previously adds little noise to the image because the number of singles recorded by each detector is so high. However, the singles method has its own difficulties, and requires measurement of  $\tau$ , which is subject to inaccuracies.

### Attenuation Correction

If 511-keV annihilation gamma rays were made to travel through a substance with a very high atomic number, such as a lead brick, only a few of the photons would pass completely through the brick unaltered [13]. Most of the photons would interact with the atoms of lead. Of those that interacted, some would do so by a process called the photoelectric effect, which involves both an atomic electron and the nucleus of the lead atom. In this process, the photon completely disappears. It is totally absorbed or “stopped” by the lead, its energy transferred to the nucleus and a fast-moving atomic electron. Other gamma rays passing through the lead brick would interact by a process called scattering (or more properly Compton scattering, after A H Compton, its discoverer). In this process, the photon strikes one of the atomic electrons surrounding the atom, the gamma ray is deflected from its original direction and continues in a new direction with reduced energy. The bigger the angle of deflection, the more energy the gamma ray will have lost. A photon undergoing such a collision is said to have scattered. In lead, the two processes—complete absorption or stopping, and scattering—are both likely. In soft tissue, complete absorption almost never occurs. Instead, essentially all interactions result in the photon scattering. Even in bone, 511-keV photons are absorbed only rarely. Instead they most simply scatter.

Now consider photons emitted by a small region of myocardium. Some small fraction of the annihilation photons will be headed in a direction such that both photons would strike a detector in the ring. As these photons travel toward the detector, they must pass through the tissue of the body. If either of the photons scatters, it will no longer be headed toward the detector. In all probability it will miss the ring entirely, or on those occasions that it does not, its energy may be too reduced to be detected. A coincident event that would have occurred in the absence of intervening tissue, now does not occur. The photons emanating from this small section of the myocardium are said to have been attenuated, and the loss of detected events due to interactions with atoms of the intervening tissue is called attenuation. The number of photons that make it through unscathed decreases exponentially

12 PART I Instrumentation, Imaging Techniques, and Protocols

with the thickness ( $d$ ) of interposed tissue:

$$\begin{aligned} &\text{Number of photons reaching the detector} \\ &= \text{Number of photons headed for detector} \times e^{-\mu d} \end{aligned}$$

The constant  $\mu$  is the attenuation coefficient and has a value of  $\sim 0.096 \text{ cm}^{-1}$  for 511-keV photons in soft tissue. As can be seen by applying the equation above, only half of the photons will make it through 7.2 cm of tissue. Lower energy photons such as those emitted by  $^{99\text{m}}\text{Tc}$  (140 keV) are attenuated more easily, because  $\mu$  is higher at lower energies. It takes only 4.6 cm of tissue to stop half the photons of  $^{99\text{m}}\text{Tc}$  from reaching their original destination. It would, therefore, seem that attenuation would be much more significant for SPECT scans than for PET scans, because the lower energy  $^{99\text{m}}\text{Tc}$  photons used for SPECT scintigraphy are so much more easily attenuated. This presumption is, however, incorrect. In a PET scan, both photons in a pair must reach their respective detectors. As illustrated in Figure 1.6a, a photon headed toward detector D1 must travel through a thickness of tissue  $X_1$  without interaction, and the photon going in the opposite direction must travel through thickness  $X_2$  to reach detector D2. The total attenuation is then:

$$\begin{aligned} &\text{Number of coincidences} \\ &= (\text{Number of photons headed for D1 and D2}) \\ &\quad \times (\text{probability photons gets to D1}) \\ &\quad \times (\text{probability photon gets to D2}) \\ &= (\text{Number of photons headed for D1 and D2}) \\ &\quad \times e^{-\mu(X_1)} \times e^{-\mu(X_2)} \\ &= (\text{Number of photons headed for D1 and D2}) \\ &\quad \times e^{-\mu(X_1+X_2)} \\ &= (\text{Number of photons headed for detector}) \\ &\quad \text{D1 and D2} \times e^{-\mu D} \end{aligned}$$

where  $D$  is the total distance,  $X_1 + X_2$ , through the body.

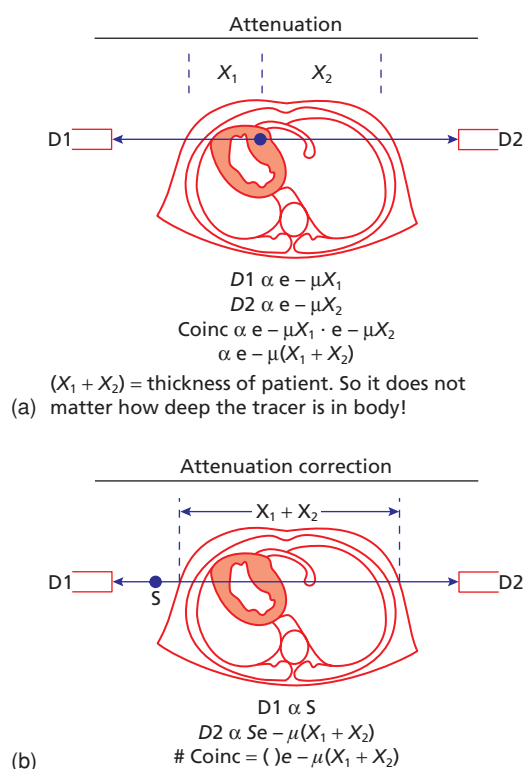


**Figure 1.6** (a) The attenuation suffered by the pair of photons does not depend on where in the body that pair of photons originated. No matter where they originate, together they have to traverse a thickness  $X_1 + X_2$  of tissue. (b) Because of this, the same attenuation is experienced by a radioactive source placed outside the body, permitting the attenuation to be measured. One simply measures the number of pairs of photons detected without the patient and compares this to the number detected when the patient is present.

Therefore the attenuation of the pair of photons depends only on  $D$ , the total amount of tissue the pair of photons has to traverse. It does not depend on where in the body the annihilation occurred. One does not need to know  $X_1$  and  $X_2$ , only the attenuation resulting from its sum,  $D$ . This is not the situation for SPECT, in which only one photon is detected. In the SPECT case one needs to know what depth (e.g.,  $X_1$ ) the photon came from. This is a piece of information that is usually unknown and unmeasurable.

For typical chest thicknesses most of the photons will be attenuated. Often only  $\sim 10\text{--}30\%$  will make it through the body. Photons traveling in

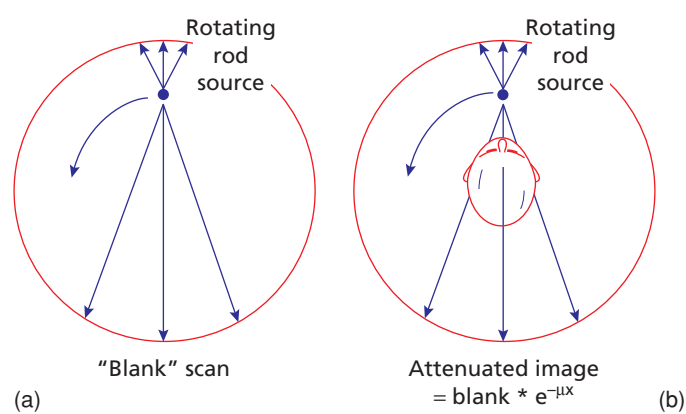
other directions toward other detectors and those originating from other sections of the myocardium may be more or less extensively attenuated. In a 70-kg subject, attenuation by factors of 5–20 is not uncommon. Attenuation can be even greater in obese subjects. Obviously, attenuation has significant effects on the results of cardiac PET scans. Although this problem is serious with PET because both photons in a pair must survive intact, accurate attenuation correction is possible. In contrast, with methods such as SPECT in which only one photon is involved, such correction is not possible because the attenuation correction factor,  $e^{-\mu(X_1)}$ , depends on measurement of the depth at which the isotope is located in tissue. This measurement cannot be made before imaging. The value necessary for attenuation correction of PET images, however, is  $(X_1 + X_2)$ . This quantity is independent of how deep the isotope is located in the body and depends only upon the attenuation through the total body thickness, which can be measured accurately. The most common method for making this measurement involves performance of a “blank” scan and an “attenuation” scan (often called a transmission scan). Figure 1.6b illustrates this approach for one detector pair [7,14]. Before the patient to be imaged is placed in the ring, a small positron-emitting source is placed at one side (as in Figure 1.6b) and the number of photons detected is recorded (just as in Figure 1.6b but without the patient). The position of the source is maintained, and the patient is positioned in the ring (before injection of the isotope) as in Figure 1.6b. Again, the number of photons are recorded. The difference in the

counts detected in the blank and transmission scans is of course caused by attenuation through the patient. For example, if  $S$  coincident counts were recorded by the detector pair shown in Figure 1.6b before the patient was in place, then  $S \times e^{-\mu D}$  counts would be recorded by the same detector pair when the patient was interposed. The ratio of the counts without the patient (called the “blank” scan counts) to the counts with the patient in place (called the “transmission” scan counts) gives the factor  $e^{+\mu D}$ , which is the factor needed to correct for attenuation for this particular detector pair. Making the same measurement for all detector pairs permits complete attenuation correction.

In order to make the measurement of attenuation for all detector pairs, often a rod of activity is used with its long dimension oriented along the  $Z$ -axis (Figure 1.7). Such a rod is attached to a mechanism that rotates it at a fixed speed around the gantry. The rod is usually filled with a relatively long lived positron emitter ( $^{68}\text{Ge}$  which decays to  $^{68}\text{Ga}$ ). The rod is first made to rotate without the patient, giving the “blank” scan counts (Figure 1.7a). Then the patient is positioned and the measurement repeated (Figure 1.7b) giving the transmission scan. The ratio of the counts in the blank to the counts in the transmission for every detector pair gives the attenuation correction factor for that detector pair.

As the rod rotates, only those detectors that lie on the line formed by the detector, the rod, and the opposing detector can possibly be in coincidence. By turning on only the appropriate detectors as the rod rotates around the gantry, most accidental and scatter coincidences can be eliminated. With proper

Figure 1.7 Illustrating [7] how the process described in Figure 1.6 can be implemented. In panel (a) the “blank” scan is taken with a source and no patient. In panel (b) the same source is used with the patient in place. For every possible pair of detectors the ratio of detected events with and without the patient is compared to compute the attenuation correction factor.



correction software, this also permits the transmission measurement to be made even after activity has been injected [15,16]. Some manufacturers use instead an isotope which emits only a single photon (e.g.,  $^{137}\text{Cs}$ ). This makes it more difficult to remove scattered events, but in general both methods have been shown to work satisfactorily. Many modern PET scanners have been combined with a CT scanner, and in this case the CT scan (after suitable processing) can be used to perform attenuation correction. This will be discussed further later in this chapter.

A typical scanning sequence is: (1) obtain a blank scan (usually only done once per day or week); (2) for static FDG imaging, inject the patient, wait for uptake (typically 1 hour) then position the patient in the gantry and obtain a transmission scan either immediately prior or immediately following the emission scan. This minimizes motion between the transmission and emission scan. For dynamic scanning, the transmission scan must be taken prior to injection (or it can be done following the scan). As mentioned above, to perform the transmission scan after injection requires that hardware and software be available for correcting for emission activity present during the transmission scan. This is fairly straightforward when positron emitters (and coincidence detection) are used for the transmission source. It is often more difficult when single photon emitters are used for the transmission source. No matter what scheme is used, it is important to prevent patient motion between the transmission and emission scans. Such motion can produce appreciable errors in the uptake image [17].

### Scatter

When annihilation photons pass through tissue, they frequently collide with electrons and scatter. The photon is deflected from its original direction and loses some fraction of its energy. The higher the angle of deflection, the greater the energy loss. The great majority of scattered photons never reach a detector, as illustrated in Figure 1.8. A small percentage of scattered photons, however, may still hit a detector in the ring and register coincidences, as shown in Figure 1.8. When this occurs, the PET camera erroneously computes the position of the radioactive atom (dotted line in Figure 1.8). Such

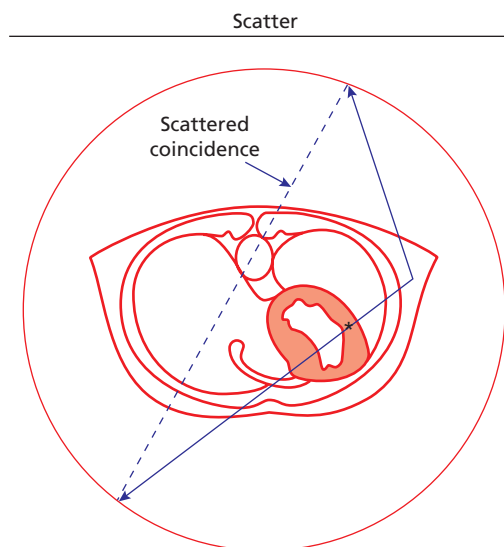


**Figure 1.8** Illustrating the effect of scattered radiation. If one of the pair of photons originating in the heart (shown as an asterisk in the free wall of the myocardium) scatters and is detected (as shown at about the 1-pm position in the detector ring), the PET scanner will erroneously think the positron was emitted along the dotted line. A "scattered coincidence" will have occurred.

mispositioning of events can cause false counts to appear in cold areas of an image when a hot region is nearby. In general, the phenomenon slightly blurs sources of radioactivity from hot regions into cold regions (even those a few cm away). This is of particular importance in cardiac imaging, since the observer is frequently trying to detect defects of uptake in segments of myocardium adjacent to normal regions (and perhaps adjacent to a hot liver).

Most PET scanners are designed to reduce the effects of scattered photons by rejecting those photons whose energy is below a certain threshold value. In most older, and some newer generation, scanners bismuth germinate (BGO) crystals are used. The energy resolution of these detectors is not very good, making it more difficult to reject scatter. Other crystal types (lutetium oxyorthosilicate (LSO) or gadolinium oxyorthosilicate (GSO)) in theory have better energy resolution, but in practice have yet to achieve much better scatter energy rejection than the new generation BGO scanners. In PET scanners with septa (2D scanners), scatter is usually fairly small anyway. However, as will be seen later,

scanners without septa (3D mode) have several times higher scatter, and so the problem is more severe. If a scanner operates with an energy threshold of 360 keV, it can reject all photons that have been scattered by more than about  $57^\circ$ , but not those scattered less than this. Because photons are more likely to scatter at small angles, a large number of scattered photons will still be detected. Attempts to raise the energy threshold to, for example, 400 keV (as is being done in some of the scanners with LSO or especially GSO crystals) would result in the rejection of photons that had scattered by more than about  $44^\circ$ , but of course the higher one raises the threshold, the larger the fraction of unscattered photons that are rejected as well. Energy rejection can, therefore, be used to reduce large-angle scattering, but can only eliminate smaller angle scattering at the expense of eliminating unscattered photons as well. This situation will improve if the energy resolution of the scanner can be improved. Meanwhile, more empirical methods must be applied to correct for the remaining scatter. Most modern scanners have relatively sophisticated algorithms for correcting for this residual scatter [25]. However, especially for cardiac imaging (with its mixture of lungs and adjacent soft tissue) the algorithms are not perfect. The situation for septa-out (3D) imaging is more problematic, and for this and other reasons (as discussed further below), there is still discussion as to whether septa out imaging might be a poorer choice than 2D (septa-in) imaging for cardiac [9–12].

### Deadtime

Quantitatively accurate PET studies require that the number of true coincidences be directly proportional to the concentration of radioactivity. In addition to physical phenomena such as scatter and accidental coincidences, a significant electronic effect in PET cameras can alter this relationship. Every time a photon produces a scintillation in a detector, a complex series of electronic events must occur: The light must be converted into an electronic pulse; the exact time of occurrence of the electronic pulse must be determined for use in timing coincidence; and the magnitude of the pulse must be computed to allow rejection of scattered events, etc. All of this takes time. If a second photon should ar-

rive before the processing of the previous pulse is complete, the second pulse may be lost. There is, therefore, a time interval after a photon has interacted with a crystal during which the PET scanner electronics may be unable to process further pulses. Pulses that occur during this interval, termed the “deadtime,” are lost. The higher the count rate, the larger will be the fraction of lost pulses. The number of coincidences/second at first increases linearly with activity, but at high activities it deviates from linearity due to this deadtime. Successive increases in activity produce successively smaller increases in coincidence rate.

The principal source of deadtime is often not the number of coincident events the machine must process per se, but rather the rate at which the system must process single photons (each one of which must be analyzed to see if it meets the energy requirements and to see if it is in temporal “coincidence” with another photon, etc.). The singles rate recorded by a detector is often one or more orders of magnitude greater than the coincident rate. Often the deadtime loss of a detector can be predicted quite accurately as a function of the singles rate measured by the detector. This relationship is the basis for one effective method for correcting for deadtime. The corrections can be quite large, especially with imaging techniques that require bolus injections of isotope (e.g.,  $^{82}\text{Rb}$ ). It is probably best to limit the amount of activity injected so that the required deadtime correction during imaging will be less than a factor of 2. Activity levels greater than this will result in increased radiation exposure to the patient without a comparable increase in true coincidences. In addition, the accuracy of larger correction factors may be suspect.

In many circumstances cardiac PET studies are especially susceptible to the effects of deadtime, particularly with septa-out (3D) scanners. This is particularly true with dynamic cardiac studies that attempt to measure the wash-in or wash-out of activity from the myocardium, or to measure arterial activity as a function of time by monitoring the activity in the atrial or ventricular cavities. During a bolus injection or even during a 1-minute infusion of isotope, the PET camera field of view may contain a large fraction of the entire injected dose. This is in marked contrast to the 60 minutes postinjection static cardiac scans in which only a small

percentage of the injected dose is in the field of view. The PET camera's deadtime characteristics (as well as random coincidences) may sometimes limit the amount of activity that can be administered. Again, the problem is far more severe when operating PET scanners in septa-out (3D) mode than in septa-in (2D) mode.

### Resolution

The term "resolution" is one of many parameters used to characterize PET scanners. The term requires more careful definition. The spatial resolution of a PET scanner is a measure of how well the scanner can distinguish two small objects placed closely together. Certain standard measurements of resolution have been adopted. With one, a very small spot of radioactivity is placed in the scanner's field of view and is imaged. If the range of the positron is very small (e.g., that of a positron from an isotope such as  $^{18}\text{F}$  embedded in plastic or aluminum), then comparison of the apparent size of the object in the image and the actual size of the object allows calculation of the scanner's resolution. However, very small point sources of radioactive material are hard to construct. Instead, often a thin rod of radioactive material, for example a long thin needle or capillary tube filled with  $^{18}\text{F}$ , may be used. Steel prevents the positrons from leaving the needle. The needle or rod is placed in the scanner, with its long axis perpendicular to the plane of the ring as shown in Figure 1.9a. Data are acquired and the image is reconstructed as shown in Figure 1.9b. The top right of the figure shows a plot of the number of coincident events as a function of distance across the image. Typically such a plot follows a bell-shaped, approximately Gaussian curve. By convention, the width of this curve at half its maximum height (full width at half maximum, or FWHM) is used as a measure of spatial resolution. Since the initial measurement is obtained within one slice, or plane, it is called the "in-plane" resolution of the scanner. The in-plane resolution will usually be somewhat larger (perhaps a few millimeters or so, depending on the scanner) when the measurement is made at the edge of the field of view, rather than at the center. Because the free wall or apex of the myocardium may be 10 cm or more from the center of the field in a cardiac PET study, it is useful to know the PET

scanner's resolution not just at the center, but also 10 or 15 cm from the center. In addition, at a given distance from the center of the scanner's field of view, the resolution in the anterior–posterior or  $Y$  direction may not be the same as that in the lateral, or  $X$  direction.

The scanner shown in Figure 1.9a is made up of crystals with a width,  $W$  length,  $L$ , in the axial or  $Z$  direction, and a depth,  $D$ . As pointed out previously the width,  $W$ , of the detectors influences the in-plane resolution. Similarly the length,  $L$ , of the detector in the  $Z$  direction determines, in part, the resolution of the scanner in the axial direction. To measure the resolution in this direction, a small "dot" of radioactive material, placed on the bed of the gantry, might be used. An image could be made of this dot of activity, the source could be moved through the gantry by 1 or 2 mm, and a second image made. Progressively moving the source of activity through the scanner in 1 or 2 mm steps, making an image at each location, would result in a series of images as a function of the  $Z$ -axis position of the source. Plotting the number of coincident events in each image as a function of the  $Z$ -axis position (clinically, the bed position), would produce a plot similar to those in Figure 1.9b. The FWHM resolution in the  $Z$ -axis direction is sometimes called the "slice thickness" because it is a measure of how far into the  $Z$ -axis the slice extends. A PET scanner, then, has at least two (possibly very different) spatial resolutions: The in-plane resolution (made up of the resolution in the anterior–posterior direction and the lateral directions,) and the  $Z$ -axis, or axial resolution.

The axial resolution, or slice thickness, should not be confused with the separation between slices. The spacing between slices may be greater or less than the "thickness" (i.e., FWHM in the axial direction) of each slice. If the spacing between slices is less than the thickness of the slice, then the slices may be considered to partially overlap. Even if the spacing between slices is greater than the slice thickness, some overlap will be present because the "edges" of a slice are not sharp but are Gaussian shaped.

The resolution of a PET image is determined by: The design of the machine (including crystal size and spacing, ring diameter, among other factors); physical factors such as the finite range of positrons

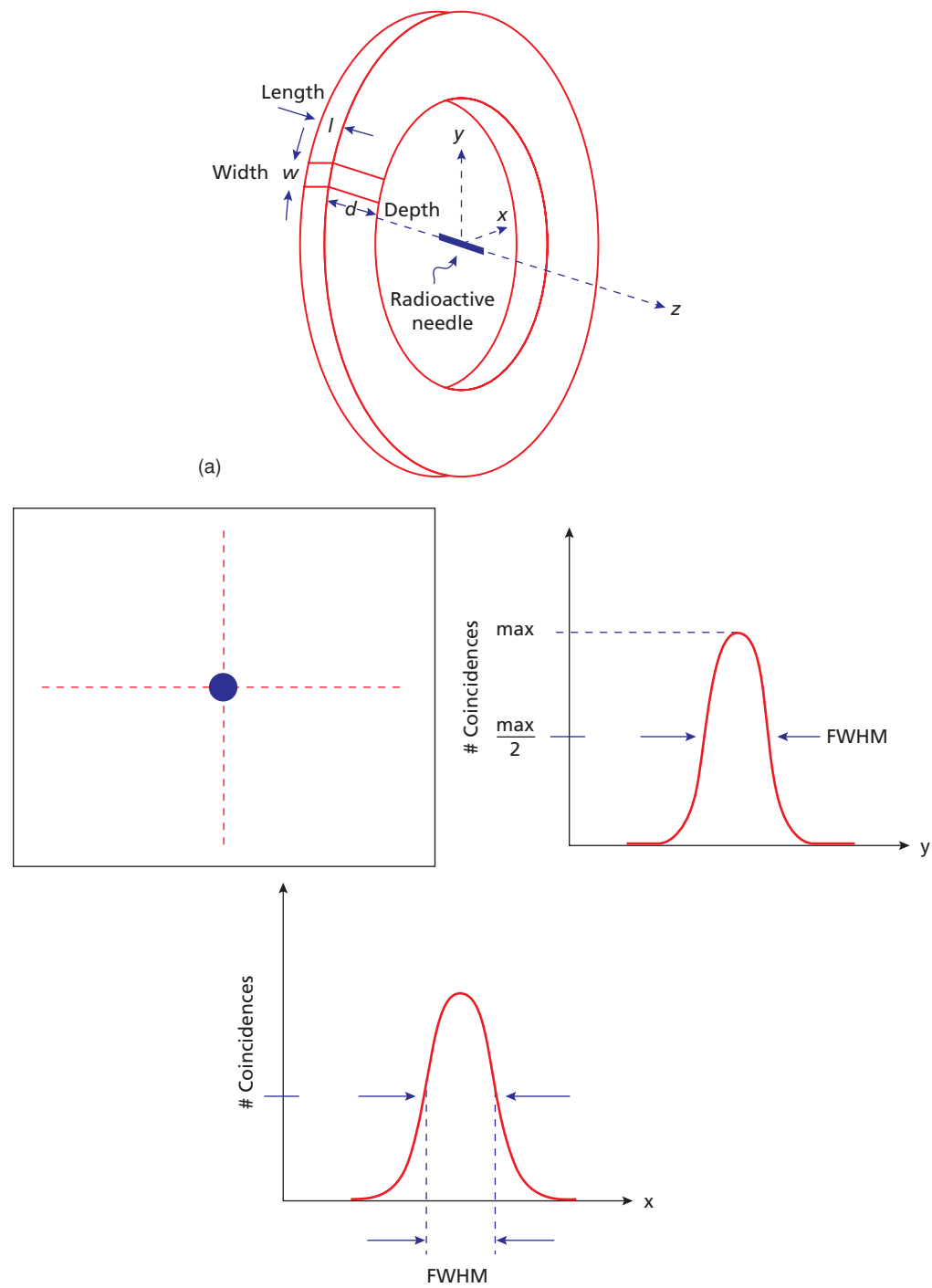


Figure 1.9 (a) Showing placement of rod source to measure in-plane resolution [7]. (b) Upper left: a transaxial image of the rod source. Upper right and lower left: profiles through the transaxial image.

in tissue and the deviation of annihilation photons from exact colinearity, and processing, including whatever smoothing is performed during or after reconstruction [19–23]. The effects of image processing are to some extent controllable. Positron range is of course a function of the isotope used. Its effects can be estimated as follows. If the number of positrons detected is plotted as a function of distance in tissue from the source, the number decreases almost exponentially with distance [20]. Some of the positrons therefore travel relatively far, altering the resolution curve from its usual Gaussian shape. The resolution curve produced by radioisotopes emitting very energetic positrons is a combination of the typical Gaussian curve illustrated in Figure 1.9b and the approximately exponential curve associated with positron penetration [21]. Therefore, the curve is roughly Gaussian in shape near the center, but exhibits a long, roughly exponential, tail. The amount of degradation in resolution that would occur with use of a positron with a relatively long range in tissue, such as  $^{82}\text{Rb}$ , can be estimated as follows:

$$\text{Final resolution} = (R^2 + 1.89 \times (2 \times D)^2)^{0.5} \quad (1.1)$$

where  $R$  is the resolution of the scanner (including any smoothing) measured with a nearly zero-range positron source (e.g., when  $^{18}\text{F}$  in a thin steel needle is used) and  $D$  is the average distance the positron travels, as shown in Table 1.1.

For example, with a scanner having 7-mm useable resolution as measured with  $^{18}\text{F}$ , the resolution expected with the use of  $^{82}\text{Rb}$  is based on the average distance an  $^{82}\text{Rb}$  positron travels ( $D$ ), 2.3 mm. The resolution of  $^{82}\text{Rb}$  scan can be calculated from the equation above to yield a final resolution of approximately 9.4 mm FWHM—a significant increase compared with that of a lower energy positron emitter. The factor of 1.89 is entered into Equation (1.1) in consideration of the fact that the number of positrons decreases with distance in an exponential rather than a Gaussian manner. Because the resolution curve is not Gaussian with an isotope such as  $^{82}\text{Rb}$ , specifying the FWHM does not tell the full story. The number of positrons decreases exponentially with distance from the source, so many positrons will travel much farther than the average. Some  $^{82}\text{Rb}$  positrons will travel more than a centimeter before annihilating.

This produces an exponential tail on the resolution curve, in turn causing a small fraction of the counts in one part of an image to blur into other, distant parts of the image. To describe this effect, the full width at tenth maximum (FWTM) is measured in addition to FWHM.

To reduce the point-to-point random statistical fluctuations (called “noise”) that are invariably present in a PET image, an image is often “smoothed” by averaging adjacent picture element (pixel) values together. Although this reduces image noise, it degrades resolution.

Various filters can be used at the time of reconstruction to facilitate smoothing. “Filtering” is the name given to the process of averaging neighboring pixels together [22] by replacing a pixel value with a weighted average of itself and its neighbors. For example, one commonly used filter replaces a pixel value with one-half times its own value plus one-eighth times each of its four nearest neighbors’ values, so that the weighting factors for this filter would be 1/2 and 1/8. Such a filter will produce a less noisy image, but one with poorer spatial resolution. Filters are often given names (e.g., the “Hanning” and “Butterworth” filters). Despite their specialized names, all filters do nothing more than average neighboring pixels together; they differ only in their weighting factors, which may be positive or negative.

In addition to filters that reduce noise but worsen resolution, filters exist that improve resolution and exaggerate noise. Unfortunately, it is a consequence of the basic laws of physics that it is impossible to simultaneously reduce noise and improve resolution, and because of statistical fluctuations caused by the limited numbers of coincident events, PET images almost always must be filtered with a smoothing, rather than a resolution-improving, filter. Some 3D small animal PET scanners are the exceptions to this rule. In these scanners there are often plenty of coincident events, because the dose/gm injected is high (dosimetry is frequently not a limiting factor in animal imaging). Resolution recovery can then be used, at the expense of slightly worsening statistical fluctuations, to achieve the higher resolution often required for small animal imaging. Some resolution recovery techniques are most easily built-in to so-called “iterative reconstruction” programs.

Clinical PET scanner software usually gives the investigator a choice of which smoothing filter to

use at the time of image reconstruction. It should be noted that iterative reconstruction techniques also have inherent “smoothing” (noise reduction combined with resolution worsening) built into them. In general, the more iterations (or iterations  $\times$  subsets) the better the resolution and the worse the noise. In addition, some filtering is often applied post-reconstruction. It is important for the user of a PET scanner to be able to estimate the resolution of the final image, given the reconstruction parameters selected. Comparing two images reconstructed with different parameters can result in misleading clinical conclusions.

It is important to clarify the difference between resolution and the distance between pixels. Imagine a PET scanner with 7 mm in-plane resolution (i.e., 7 mm FWHM) and a 41 cm in-plane field of view. The reconstructed image could be stored in an array (i.e., a digitized image) of  $256 \times 256$  pixels. Each pixel would be 41 cm/256 or 1.6 mm apart. The 7 mm FWHM would therefore correspond to about 4.4 pixels. If instead the reconstructed image were stored in a  $512 \times 512$  matrix, each pixel would comprise 41 cm/512 or 0.8 mm. The resolution would remain 7 mm FWHM which, with this matrix size, would be represented by 8.8 pixels. Resolution is a function of the scanner and the reconstruction and filtering processes; it cannot be improved by increasing the number of pixels in the image matrix. Below a certain number of pixels/centimeter, however, the image will no longer be able to reflect the resolution inherent in the scanner. In general, with PET images acquired in vivo, at least three pixels should be available for every FWHM [3]. So for example, if the final resolution of the image is to be 9 mm, then the pixel size must be 3 mm or smaller.

Pixels are spaced a fixed distance apart in the  $x$  and  $y$  direction and so occupy an area. Nearly all scanners are of course multislice machines. A pixel, then, can also be thought of as occupying a volume in space, in which case it is referred to as a voxel.

### Partial Volume Effect

Quantitative data are usually extracted from PET images with the aid of regions of interest (ROIs) drawn on the images. Analysis of the data contained in such regions yields either the total number of events/second occurring within the region (proportional to the total activity in the region), or

the mean number of events/second/voxel (proportional to the average concentration of activity in the region). Sometimes the maximum value within the ROI is also used. The resolution of the PET scanner, the size and placement of the region of interest, and the true anatomic size of the structure imaged all influence the accuracy of such measurements. Collectively, such influences are often described by a parameter called the partial volume effect [23,24].

To better understand what the partial volume effect is, assume that a “perfect” PET scanner exists, and it is used to image a 2-cm diameter cylinder of radioactivity. Assume further that after imaging for 100 seconds, 100,000 coincident events would be detected (therefore 1000 events/second) in a transaxial slice of the cylinder. The perfect scanner would produce an image like the one shown in Figure 1.10a. All pixels within the cylinder would have nearly the same value (apart from small statistical fluctuations which we will ignore), and all pixels outside it would have the value zero. Placing a 2-cm diameter region of interest around the image of the cylindrical object would give the total number of coincidences/second coming from the object (i.e., 1000 coincidences/second). All of the coincidences that were detected would occur within the region of interest.

If the same 2-cm diameter cylinder of radioactivity were imaged with an imperfect PET scanner (e.g., one with 7 mm FWHM resolution), the same 100,000 coincidences (or 1000/second) would be detected, but some of the coincidences would be blurred or spread outside the true dimensions of the cylinder (Figure 1.10b). Pixels near the center of the cylinder would not be affected as much because just as many counts would be blurred out as blurred into them from neighboring pixels, whereas pixels near the edge would be particularly affected. The same 2-cm diameter region of interest (shown as a dashed circle in Figure 1.10b) would now produce a value of only 785 events/second, the other 215 coincident events/second being spread out over pixels outside of the region of interest. The percentage of the counts retained in the region of interest is termed the “recovery coefficient”: 785 of 1000 or 78.5% in this case.

The term “partial volume effect” describes this effect [23,24]. The poorer the resolution, the more blurred the data will be and the smaller the fraction of counts “recovered” within a given region

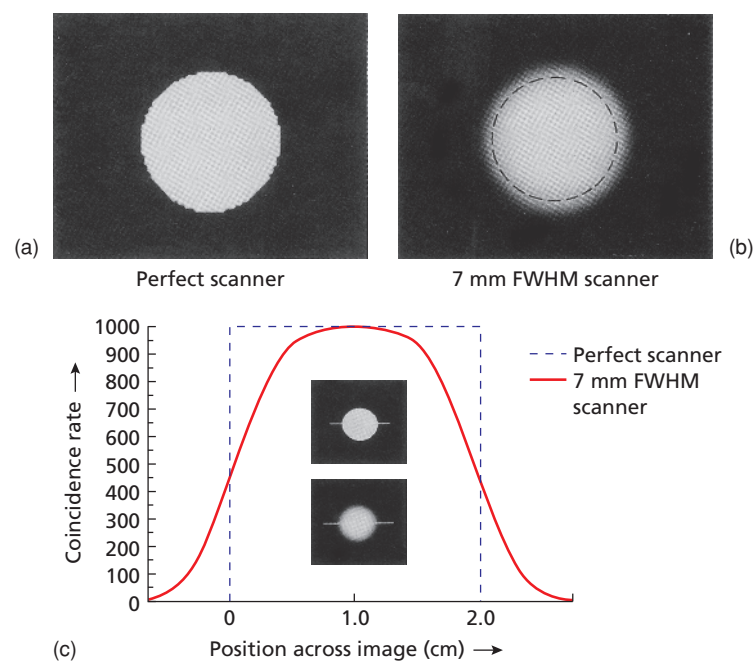


**Figure 1.10** (a) A transaxial image of a 20-cm diameter uniform cylinder, taken with a "perfect" PET camera. (b) The same image taken with a real PET scanner, with 7 mm FWHM resolution. Note the blurry edges. (c) Line profile through the ideal image (dashed line) and through the real image (solid line). A region of interest (as shown

in (b)) would recover only a portion of the activity in the image—the remaining activity would have blurred outside the region. The y-axis is a relative scale proportional to the counts/second at each pixel in the profile. FWHM, full width at half maximum.

of interest will be. As can be seen in Figure 1.10, a larger fraction of the total events can be recovered by enlarging the region of interest to more than the true 2 cm object size. If the region of interest were increased to 2.4 cm, 914 of the original total 1000 events/second would be recovered. If the region were sufficiently large, all the original events would be recovered. Unfortunately, in patients, the size of the region drawn may be limited by the presence of substantial amounts of activity in structures close to the organ being imaged.

In the discussion so far, it has been tacitly assumed that the only quantity of interest is the total activity in the region, or the total number of events/second occurring in the "organ" (in this case, the cylinder). More commonly, the average concentration of activity within a region is sought and so the counts/second/number of pixels in the ROI is measured. This is in fact the unit most commonly produced by PET scanners (usually converted to MBq/cc).

We must now reconsider what impact the partial volume effect will have on accuracy of

measurements of average concentrations of activity within an ROI. Drawing "too large" a region in an effort to recover all the counts will actually have the opposite effect on mean activity concentration measurements. It will reduce the measured counts/second/pixel by increasing the total number of pixels. Again, consider the 2-cm diameter cylinder shown in Figure 1.10b. The "ideal" PET scanner might, for example, yield 1000 events/second total within the 2 cm diameter. Let us also suppose that this value could be converted to a concentration of activity of perhaps 5 nCi/mL. The ideal PET scanner would, therefore, yield a value of 5 nCi/mL at every pixel within the 2 cm diameter, and zero outside. The mean value within any region of interest of 2.0-cm diameter or smaller would give the same value of 5 nCi/mL. If the region were enlarged to more than the true size of the object, however, the measured nanocuries/milliliter would fall because the region of interest would begin to include some pixels with 0 nCi/mL. For the 7 mm FWHM PET scanner producing the image in Figure 1.10b, the 2.0-cm region of interest would yield too low a

value for concentration of activity because events near the edge of the object would smear out to pixels outside the region. For the situation depicted in Figure 1.10, the drop would be from 5 to 3.9 nCi/mL, again with a recovery coefficient of 78.5%. If the region of interest were decreased in size, however, it would no longer include pixels near the edge and the concentration of activity would approximate the correct value of 5 nCi/mL. If the region of interest were 1.8 cm in diameter, the average counts/second/pixel would correspond to 4.3 nCi/mL (85% recovery), and if the region of interest were decreased still further to 1.6 cm, the value would be 4.5 nCi/mL (90% recovery). For measurements in nanocuries/milliliter or counts/second/pixel then, as the region of interest gets smaller, the average value within the region approaches the correct value.

Unfortunately, as the region of interest gets smaller, so does the total number of events contained in it, causing statistical fluctuations (the standard deviation) to increase. Conversely, if the region of interest is too large (larger than the object being imaged), the mean “nCi/mL” value drops. A rule of thumb is that if the edge of the region of interest is more than 2 FWHM interior to the object’s anatomic borders, the influence of the partial volume effect will be small. Unfortunately, myocardial walls are typically no thicker than 1–2 cm (except in certain disease states), whereas FWHMs are typically no less than 0.7 cm. It will often be impossible to draw a region that is even one FWHM from both epi- and endocardial borders. Accordingly, myocardial PET images are significantly influenced by partial volume effects. In general, recovery coefficients are significantly less than 100%. Even worse, since the myocardial wall varies in thickness around the heart, the thinner regions will artifactually appear to have lower activity than thick regions, even when the true underlying concentration is homogeneous.

In summary: (1) To measure only the total activity within an organ, the region of interest should be drawn very generously around the whole organ being imaged. This can only be done if there are no nearby structures containing activity. Ideally, edges of the region of interest should be at least two FWHM larger than the true organ borders. This will lead to recovery of nearly all events that have “blurred out” of the organ; (2) To measure

radioactive concentrations within an organ rather than simply total activity: (a) the edges of the region should ideally be interior to the edges of the organ by two FWHM (this is of course often impossible); otherwise, recovery will be flawed, and (b) thin myocardial walls will in general give lower recovery than thick walls. The above discussion was focused on drawing regions within a slice. However, it should be remembered that partial volume effects occur in all three directions. The same considerations mentioned above for the x and y directions, also apply to the z direction.

It has been assumed that the activity concentration is uniform within the region of interest. If this is not the case, results should be interpreted with care because the mean value within a region of interest will depend on the position of the region within the heterogeneous structure.

It is possible to correct for the partial volume effect [24]. If the true anatomic dimensions of the object being imaged and the resolution of the PET scanner (and reconstruction process) producing the image are known, it is possible to calculate the recovery coefficients and use them to correct the data. Unfortunately, the effects of cardiac wall motion also come into play. Sections of myocardium may move into and out of a region of interest as the ventricle contracts. Wall motion therefore produces its own “blurring” which influences the partial volume effect in exactly the same way as does the “real” blurring (i.e., the resolution) of the scanner itself.

## 2D versus 3D PET scanners

The PET scanners described above consist of separate rings of detectors, each of which is separated by a thin strip of high atomic number material (e.g., lead, tungsten), called the septum, Figure 1.11a. The septa act as a sort of coarse collimator. The purpose of the lead septa between rings is to reduce the number of scattered photons seen by the detector, as shown in Figure 1.11a, line “D.” In addition, the septa reduce the number of photons from out of the field of view (e.g., from the bladder) which can hit the detectors, Figure 1.11a, line “A.” With the septa in place, only coincidences from crystals in the same ring (or a few adjacent rings) of detectors will be admitted. So the pair of annihilation photons “B” do not make it through the septa,

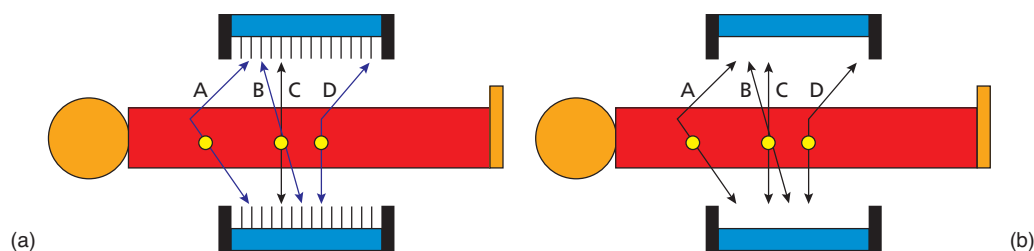


**Figure 1.11** (a) Illustrating a multislice PET camera with septa (misleadingly called a “2D” scanner). The septa stop scattered photons, like (D), out of field photons like (A) as well as valid photons that happen not to produce coincidences within the crystals in a single ring (or nearby rings). Only photon pair (C), shown in black, is detected.

(b) The same scanner operating in “3D” mode, i.e., without the septa. Now both valid photons (B) and (C) are detected, increasing the sensitivity. However, this is at the expense of detecting lots of nonvalid photons such as the scattered pair (D) and the out of field photon (A). (figure re-drawn from Bacharach [26].)

while the annihilation pair of photons “C” do. As mentioned above, this mode of operation, with the septa in place, is called “2D” mode, or “septa-in” mode. The name “2D” is slightly misleading, since the data from a multislice PET scanner operating in 2D mode, is of course 3D. The nomenclature refers to the fact that the lead septa attempt to keep out any photons not originating from within a single detector ring (or a few adjacent rings). Together, the septa, combined with the limited energy discrimination, are able to reduce scatter in heart scans to about 10–15%—a quite clinically acceptable number. This remaining small scatter is easily, albeit approximately, corrected for by using software algorithms [25].

The interslice septa not only reduce scatter, but also reduce sensitivity. By restricting the coincidences to within a single ring or pair of adjacent rings, one has eliminated not only scattered photons, but also many of the photons that might have given valid coincidences between non-neighboring rings, for example line B in Figure 1.11a. Typically, by using the scatter reducing septa, sensitivity for coincident photons is reduced by about a factor of 3–7 (depending on scanner design) compared to the situation if the septa had not been present. This is not nearly as big a reduction as incurred in SPECT by using a collimator (typically a SPECT collimator might reduce sensitivity by a factor of 1000 or more). Therefore even with the lead septa between rings, PET is still very much more sensitive than SPECT. This is because SPECT requires a honeycomb of lead holes as its collimator, since the function of the SPECT collimator is to permit deter-

mination of the direction of the incident photons. PET uses coincidence detection to determine the location of the gamma rays, in principle requiring no collimator.

PET scanners with septa (i.e., 2D mode) actually work quite well for cardiac imaging. The sensitivity, despite the septa, is sufficient to obtain good quality images using 10–15 mCi FDG injections with 5–15 minutes of acquisition time. The septa keep random events and deadtime at acceptable levels, even for high-dose studies, such as 40–50 mCi  $^{82}\text{Rb}$  injections (imaging 90 seconds postinjection), or 20 mCi  $^{13}\text{N}$ -ammonia injections. This is true even for relatively slow crystals such as BGO. The septa are able to accomplish this because random events (and deadtime) are greatly affected by the number of “singles” events/second. That is random events are determined by the count rate for individual detectors, rather than by the coincident count rate. The presence of the septa greatly limits the number of singles events/second, making 2D imaging advantageous for high-activity studies. The use of septa, then, greatly reduces scatter, as well as random and deadtime corrections.

Despite the good performance of current generation 2D scanners for cardiac imaging, the need to perform whole-body oncology scans made manufacturers look for ways to increase sensitivity. Cardiac imaging would also benefit from a sensitivity increase, provided it could be accomplished without sacrificing other machine characteristics important to cardiac imaging. A gain in sensitivity would permit either shorter imaging time (less of an issue for cardiac imaging than for whole-body

imaging), or increased total counts (useful for producing gated images), or better dosimetry, or some compromise between these factors.

Most new generation scanners have attempted to increase sensitivity by removing the septa, and operating in “3D” mode [26–29], Figure 1.11b. However, removing the septa greatly increases scatter, increases the effect of out of field activity, greatly increases randoms, and greatly increases the potential for deadtime. Comparing Figure 1.11a and Figure 1.11b illustrates why this is so. In 2D mode (Figure 1.11a) only one of the four photon pairs (the black one) was detected. In Figure 1.11b all four were detected. Only two of them (B and C) actually carry valuable information.

Typically, removal of the septa increases scatter in cardiac imaging to 50% or more for large subjects. Software to correct for scatter is available, but the accuracy of the correction is not nearly as good in 3D mode as in 2D mode for thoracic imaging, and of course the magnitude of the necessary correction is many times bigger for 3D mode than 2D. Scatter is especially important when imaging cold areas near hot regions, such as a defect surrounded by normal uptake tissue. In such situations, scatter artifactually increases the counts in the defect region. If the scatter correction algorithm is not perfect, the defect size and extent can be significantly biased. Scatter correction is thought to be slightly less important for hot spot tumor imaging, but of course even in this situation, scatter can result in inaccurate quantitation, or even artifacts. It was hoped that the better energy resolution of the newer crystal types (e.g., LSO and GSO) might greatly reduce the additional scatter caused by removing the septa. While these detectors have slightly improved the scatter problem, they have not yet proven to be the panacea originally hoped for. On the other hand, the faster response time of these new crystals was successful in reducing random events by roughly a factor of 1.5–2.

Despite the difficulties, the removal of the septa seems to have been clinically acceptable for oncology imaging—the reduced scan time compensating for a greater difficulty in quantifying uptake. For cardiac imaging much work is still being done to determine under what circumstances 3D imaging might be acceptable. Certainly it will be useful when dosimetry considerations dictate a low

injected dose (e.g., for multiple sequential studies), or if only limited amount of the tracer was available (e.g., for some hard to produce radiopharmaceuticals). For static FDG imaging it may well prove perfectly acceptable (providing scatter can be adequately corrected). For dynamic imaging (e.g., bolus injections of  $^{82}\text{Rb}$  or  $^{13}\text{N}$ -ammonia) 3D imaging is more problematic. Much work is needed to determine the optimum activity levels that will be acceptable for 3D scanners, and whether 2D or 3D imaging is better in such circumstances. This is very important work, because many current generation scanners can only function in 3D mode (i.e., the septa cannot be inserted or retracted at will).

An additional problem with removing the septa is that the axial sensitivity rapidly decreases from a maximum at the center of the axial field of view, to the end slices. This is because in 3D coincidences are allowed between many rings of detectors, as in Figure 1.11b. This is fine in the center of the field, but as one approaches the edge of the field of view, there are fewer and fewer adjacent rings, causing the sensitivity to drop. This loss of sensitivity at the edges means that the effective overall sensitivity is not as high as one might predict. For oncology studies it means that significant overlap must occur between the axial fields of view at each imaging location. For cardiac studies it simply means that the noise will increase rapidly for slices further from the center of the axial field of view.

### PET Time of Flight Imaging

Recently machines have been introduced which incorporate “time-of-flight” information in the acquisition process. Time of flight refers to measuring the precise time difference between the times the two 511-keV annihilation photons are detected. In Figure 1.4 it is assumed that the photon that hits detector A also hits B “simultaneously,” where by “simultaneously” we mean that the two events occur within the resolving time of the coincidence circuits. This resolving time is relatively coarse. Obviously, since detector A is closer to the origin of the photons than detector B, in theory detector A would see the photon slightly sooner than B. However, as the photons travel at the speed of light this time difference is much smaller than the resolving time

of most current generation PET scanners. The coincidence between A and B then only tells us that the annihilation (and therefore the radiotracer) lies somewhere along the line between A and B. It does not tell us where along that line the annihilation occurred. To determine where along the line the radiotracer lies, we need to examine all the coincidences from all detector pairs, and then reconstruct the data. If, however, one could measure this small time difference between when detector A was struck compared to when detector B was struck, it would be possible to determine exactly where along the line the photon originated, making reconstruction unnecessary. Unfortunately, current detector and instrumentation technology is not nearly good enough to achieve this accuracy of time measurement. Still, some new machines are able to roughly measure this time difference, and so pin down the approximate location of where the annihilation occurred along the coincidence line, at least within 10s of cm. Such approximate information unfortunately is insufficient for avoiding the reconstruction process. But by adding even such crude timing information, it should be possible to improve the statistical quality of the data (i.e., the noise), and perhaps in the future reduce scatter. Machines with this ability have only recently been introduced, so their clinical utility is at present unclear. Still, as electronics (and perhaps detectors) get faster, this approach may prove useful. It should be noted that the idea of adding "time-of-flight" information to PET scanners is actually quite old. But only recently has the idea been revisited.

### Use of PET/CT in Cardiology

The vast majority of new PET scanners being sold today are combined with a CT scanner. The CT scan can be used to replace the much slower rotating  $^{68}\text{Ge}$  rod source transmission scan thereby reducing scan time by 3–6 minutes/field of view. In addition the rotating rod transmission source, due to limited counts, introduced noise into the corrected PET images. The CT images are by comparison nearly noise free. The two scanners are physically located in the same gantry, but do not perform scans simultaneously. Instead one usually first acquires (for oncology) a rapid spiral CT scan (perhaps 20 seconds for a head to thigh scan) and then

the much slower PET scan (several minutes/bed position). With the rotating rod source method scans of 4–6 minutes/bed position were commonly used. This resulted in 24–36 minutes of extra scan time for a six-bed position oncology whole-body scan. With CT this is reduced to ~20 seconds. In addition it soon became clear that much valuable clinical information was present in the fused CT and PET images.

Transmission scan time is much less an issue with cardiac scans, because they are acquired at a single bed position. The reduced attenuation correction noise would, however, be beneficial. In addition, it is possible that combining CT cardiac data with PET metabolic or perfusion data, as obtained from PET/CT machines, will be of clinical value. There have been several reports in the past of the clinical utility of fusing coronary angiograms with SPECT perfusion data. Recently 64 slice CT scanners have begun to be marketed with PET scanners. Many of these scanners are fast enough to permit CT cardiac gating, and will even operate with commercially available CT coronary angiography software. Many of the other cardiac CT procedures (aside from angiography) that could be used with PET often still involve contrast media. For example, even with very low concentrations of contrast media in the blood, it is reasonably easy to identify the endo- and epicardial borders using gated CT images. Thus one could correct the PET data for any partial volume effects, for example caused by thinning of one part of the myocardium compared to another. In addition, while gated FDG PET is adequate for global measures of ventricular function [30–36], the gated CT would also allow measurement of myocardial thickening—a very useful adjunct to PET physiologic (metabolic or perfusion) imaging.

Unfortunately, there are at present some unresolved issues associated with using a high speed CT scan for attenuation correction of cardiac images. A few of these are discussed briefly below.

### Use of CT Images for Attenuation Correction

As described above, when using a PET scanner, transmission related noise can be nearly eliminated by using the CT data to perform the attenuation correction. The physics of the process has been described in detail previously [37–40]. In short, a

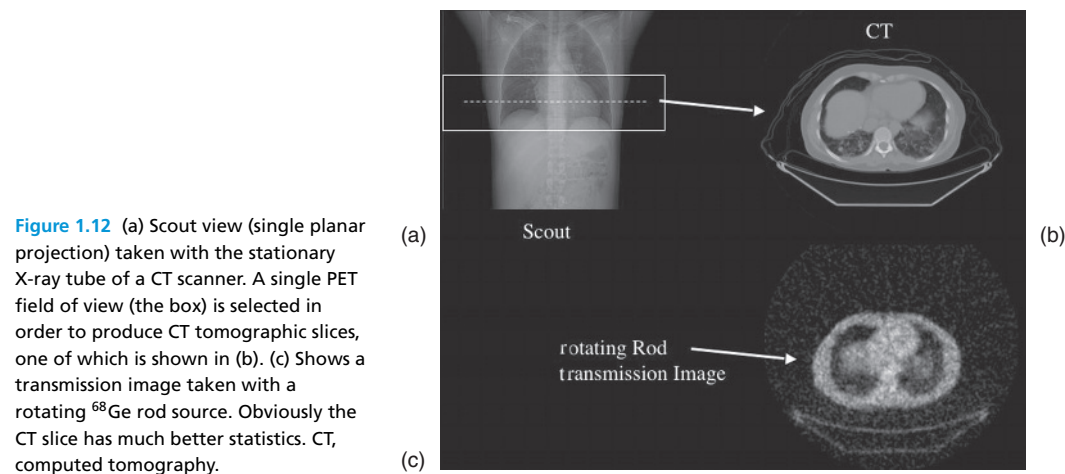


**Figure 1.12** (a) Scout view (single planar projection) taken with the stationary X-ray tube of a CT scanner. A single PET field of view (the box) is selected in order to produce CT tomographic slices, one of which is shown in (b). (c) Shows a transmission image taken with a rotating  $^{68}\text{Ge}$  rod source. Obviously the CT slice has much better statistics. CT, computed tomography.

CT scan is taken of the patient immediately prior to the PET scan. Usually a quick scout acquisition is first taken, and from this scan, one can accurately position both the axial CT scan, and the subsequent PET imaging, over the cardiac chambers. Typical images are shown in Figure 1.12. The CT scan is assumed to be aligned with the subsequent PET scan, just as the conventional transmission scan obtained with a  $^{68}\text{Ge}$  rod source is assumed to be aligned. The CT scan, even at relatively low exposure settings (e.g., 140 kVp, 80 mA, 1.5 pitch, rotation speed of 0.8 seconds) has far less noise than does the typical  $^{68}\text{Ge}$  rod source transmission scan (Figure 1.12). The CT scan is resampled to the same size as the PET data, is suitably blurred, and scaled [26] so as to convert the pixel values from Hounsfield units to the attenuation coefficients, which would be obtained at 511 keV. The scaled, resampled CT data is then used to correct the PET data prior to reconstruction.

This procedure works reasonably well for oncology whole-body imaging, although there are some difficulties. Some of these difficulties are potentially exacerbated when the process is applied to cardiac imaging. There is a small but growing body of literature concerning the accuracy and reliability of the CT attenuation correction for tumor imaging [37,41,42]. There is a growing body of corresponding data validating the method for cardiac imaging [39,43,44].

The two principal areas of concern for CT attenuation correction in cardiac PET are listed below:

**1** Scaling the CT Hounsfield units to 511-keV attenuation coefficients.

The X-ray beam from the CT scanner is of much lower energy than the 511-keV photons being imaged. In addition, the X-ray beam produces a continuous spectrum of energies all the way up to the peak (kVp). The attenuation of these lower energy CT photons is therefore much greater than the attenuation experienced by the 511-keV annihilation photons. To correct for this the attenuation values produced by the CT scanner have to be converted to 511-keV attenuation values. This aspect of PET/CT has been well validated in oncology imaging, and has been shown to work quite well in general [37,41,42], with only a few caveats. The only potential difficulties that might occur during cardiac imaging are if contrast media has been used during or prior to the CT scan [42,45–49], or if metallic objects (e.g., clips, shoulder or arm prostheses) are in the plane of the cardiac images. When arms are not up (i.e., arms at the side), some artifacts and noise can be introduced into the CT scan. There may also be some small concern caused by the proximity of the myocardium to the ribs.

**2** Misalignment between CT and emission data

Misalignment between the CT data and the PET data is a potential problem when using CT data to perform attenuation correction for PET. The misalignment can be inadvertent (i.e., patient motion between the time of the CT and emission acquisitions) or “effective” misalignment due to patient respiration and myocardial motion during the

cardiac cycle. We assume here that the PET and CT portions of the machine itself have been previously determined to be in accurate mechanical alignment.

The effects of a misalignment between the attenuation scan and the emission scan have already been investigated for PET [17]. Prior to PET/CT the only cause of this misalignment was whatever inadvertent patient motion might have occurred between the two scans. Relatively small misalignments can cause a myocardium with uniform uptake to appear nonuniform. In PET/CT the misalignment comes not only from inadvertent patient motion, but also from the motion of the internal organs caused by respiration. The CT scan is usually acquired quite rapidly, perhaps taking less than 1 second/slice. The CT therefore captures the chest at one phase of the respiratory cycle. The PET emission data, on the other hand, is acquired over many minutes, and so is an average over many respiratory cycles. The two data sets therefore do not overlay each other. The problem is most severe at the boundaries between low and high attenuation regions. For oncology studies this is usually at the dome of the liver. For heart studies it is all regions of the myocardium surrounded by lungs. In addition, not only does the heart itself appear to move with respiration, so too does the liver. As the liver moves into or out of the cardiac slices, the attenuation for those slices can change substantially. Figure 1.13 illustrates the effect, showing a CT slice captured at normal tidal end-inspiration and normal tidal end-expiration.

Several studies have examined the effects of respiratory motion on PET/CT in oncology [50–55] and it is useful to consider how those findings might apply to cardiac imaging. In oncology applications, one of the most notable effects is at the dome of the liver, where respiratory motion is large and there is an air-tissue interface. In one study [55], nearly all (84%) subjects exhibited a cold artifact at the top of the liver, with 16% of the subjects having a defect categorized as moderate. The source of the defect was thought to be the incorrect attenuation correction, due to inconsistencies at the lung/liver interface in the CT compared to the emission PET. Similar effects occur with the free wall of the heart [43,56]. A tissue/lung interface exists, and there is indeed respiratory motion (as well as cardiac motion, depending on the speed of the CT scanner). The magnitude of such effects in the heart can be significant [43]. Previous results describing the effects of misalignment between attenuation and emission data are germane [17]. Much work remains to be done in using CT images to correct for attenuation. One solution would be to slow down the CT scan (using very slow rotations and low mA) so as to average a few respiratory cycles together [57,58]. While this may lengthen the scan unacceptably for multilevel oncology imaging, it should be quite practical for cardiac imaging. It can, however, produce artifacts in the CT data. Another excellent solution that has been put forth, is to acquire a very low dose CT cine of the heart over 1 or more respiratory cycles, and then average the cine frames together. This avoids the CT artifact problem. Still

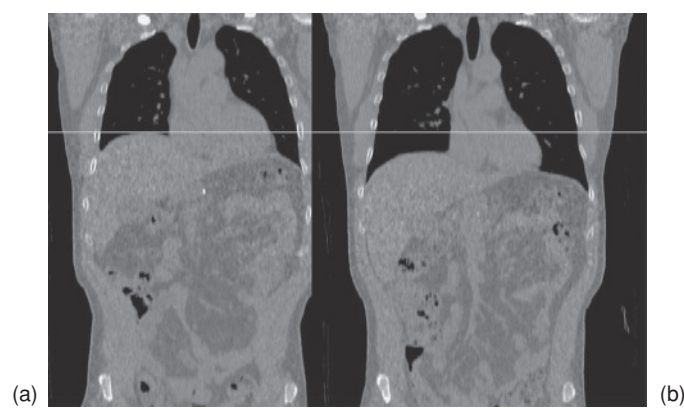


**Figure 1.13** Two coronal CT views at exactly the same level: (a) taken at normal end-expiration; (b) at normal end-inspiration. Note movement of the dome of both the liver and the heart.

another solution would be to use respiratory gating or even 4D imaging [50]. All of these solutions at present may add considerable complexity to the acquisition, but manufacturers are rapidly realizing the necessity for making such corrections in a clinically feasible fashion.

It should be noted that many CT scanners routinely scan fast enough to capture only a portion of the cardiac cycle itself. Again, problems similar to those described above may occur. Here, however, the motion (and so potential misalignment) is presumably smaller. In addition only a minimal reduction in CT scan speed would average several cardiac cycles together.

In summary, combining CT with PET imaging is likely to prove even more valuable for cardiac imaging than for oncology imaging. The additional information associated with overlaying physiologic data (metabolism, blood flow, etc.) with CT angiographic data, coupled with wall thickness and thickening measurements would seem to portend significant advances in the field of cardiac imaging. However, the problems associated with respiratory motion are likely to be much worse for cardiac imaging than for oncology imaging. Considerable work has been done to address these problems, and cardiac PET/CT is rapidly achieving its full potential.

## References

1. ICRP. *Radionuclide Transformations*. New York: Pergamon Press, 1983.
2. Dilsizian V. *Myocardial Viability: A Clinical and Scientific Treatise*. New York: Futura Publishing Company, Inc., 2000.
3. Bacharach SL, Bax JJ, Case J, et al. PET myocardial glucose metabolism and perfusion imaging: part I – guidelines for patient preparation and data acquisition. *J Nucl Cardiol*. 2003;10(5):545–556.
4. Lederer CM, Shirley VS. *Table of Isotopes*, 7th edition. New York: Wiley, 1978.
5. Parker J. *Image Reconstruction in Radiology*. Boca Raton: CRC Press, 1990.
6. Maass RE, Bacharach SL. Imaging Instrumentation. In: Iskandrian AE, Verani MS (eds). *Nuclear Cardiac Imaging: Principles and Applications*. New York: Oxford press, 2003, pp. 28–50.
7. Bacharach SL. The physics of positron emission tomography. In: Bergmann SR, Sobel BE (eds). *Positron Emission Tomography of the Heart*. Mount Kisco, NY: Futura Publishing Co., 1992, pp. 13–44.
8. Bacharach SL. The new generation PET/CT scanners: implications for cardiac imaging. *J Nucl Cardiol* 2004;11: 388–392.
9. Knesaurek K, Machac J, Krynycky BR, et al. Comparison of 2-dimensional and 3-dimensional Rb-82 myocardial perfusion PET imaging. *J Nucl Med*. 2003;44(8): 1350–1356.
10. Knesaurek K, Machac J, Krynycky BR, et al. Comparison of 2D and 3D myocardial PET imaging. *J Nucl Med*. 2001;42(5):170.
11. Machac J, Chen H, Almeida OD, et al. Comparison of 2D and high dose and low dose 3D gated myocardial Rb-82 PET imaging. *J Nucl Med*. 2002;43(5):777.
12. Votaw JR and White M. Comparison of 2-dimensional and 3-dimensional cardiac Rb-82 PET studies. *J Nucl Med*. 2001;42(5):701–706.
13. Murphy PH. Radiation Physics and Radiation Safety. In: Iskandrian AE, Verani MS (eds). *Nuclear Cardiac Imaging: Principles and Applications*. New York: Oxford University Press, 2003, pp. 7–27.
14. Bacharach SL. Attenuation correction: practical considerations. In: Schwaiger M (ed.). *Cardiac Positron Emission Tomography*. Boston: Kluwer Academic Publishers, 1996, pp. 49–64.
15. Carson RE, Daubewitherspoon ME, Green MV. A method for postinjection pet transmission measurements with a rotating source. *J Nucl Med*. 1988;29(9): 1558–1567.
16. Thompson CJ, Ranger NT, and Evans AC. Simultaneous transmission and emission scans in positron emission tomography. *IEEE Trans Nucl Sci*. 1989;36(1):1011–1016.
17. McCord ME, Bacharach SL, Bonow RO, et al. Misalignment between pet transmission and emission scans – its effect on myocardial imaging. *J Nucl Med*. 1992;33(6): 1209–1214.
18. Bendriem B, Soussaline F, Campagnolo R, et al. A technique for the correction of scattered radiation in a pet system using time-of-flight information. *J Comput Assist Tomogr*. 1986;10(2):287–295.
19. Hoffman EJ, Phelps ME. Resolution limit for positron – imaging devices – reply. *J Nucl Med*. 1977;18(5):491–492.
20. Evans R. *The Atomic Nucleus*. New York: McGraw-Hill, 1955, pp. 625–629.
21. Phelps ME, Hoffman EJ, Huang SC, et al. Effect of positron range on spatial-resolution. *J Nucl Med*. 1975; 16(7):649–652.
22. Bacharach SL. Image analysis. In: Wagner HN, S Z, Buchanan JW (eds). *Principles of Nuclear Medicine*. Philadelphia: W.B. Saunders, 1995, pp. 393–404.

28 PART I Instrumentation, Imaging Techniques, and Protocols

23. Hoffman EJ, Huang SC, Phelps ME. Quantitation in positron emission tomography: effect of object size. *J Comput Assist Tomogr.* 1979;3:299–308.
24. Soret M, Bacharach SL, Buvat I. Partial volume effect in PET tumor imaging. *J Nucl Med.* 2007;48:926–931.
25. Bergstrom M, Eriksson L, Bohm C, et al. Correction for scattered radiation in a ring detector positron camera by integral transformation of the projections. *J Comput Assist Tomogr.* 1983;7(1):42–50.
26. Bacharach SL. The new generation PET/CT scanners: implications for cardiac imaging. In: Zaret BL, Beller GA (eds). *Clinical Nuclear Cardiology: State of the Art and Future Directions.* Philadelphia: Mosby, 2005.
27. Muehlelehner G, Karp JS, Surti S. Design considerations for PET scanners. *Q J Nucl Med.* 2002;46(1):16–23.
28. Alessio AM, Kinahan PE, Cheng PM, et al. PET/CT scanner instrumentation, challenges, and solutions. *Radiol Clin North Am.* 2004;42(6):1017.
29. Surti S, Karp JS, Kinahan PE. PET instrumentation. *Radiol Clin North Am.* 2004;42(6):1003.
30. Schaefer WM, Lipke CSA, Nowak B, et al. Validation of an evaluation routine for left ventricular volumes, ejection fraction and wall motion from gated cardiac FDG PET: a comparison with cardiac magnetic resonance imaging. *Eur J Nucl Med Mol Imaging.* 2003;30(4):545–553.
31. Rajappan K, Livieratos L, Camici PG, et al. Measurement of ventricular volumes and function: a comparison of gated PET and cardiovascular magnetic resonance. *J Nucl Med.* 2002;43(6):806–810.
32. Machac J, Mosci K, Almeida OD, et al. Gated rubidium-82 cardiac PET imaging: evaluation of left ventricular wall motion. *J Am Coll Cardiol.* 2002;39(5):393A–393A.
33. Khorsand A, Graf S, Pirich C, et al. Gated cardiac PET for assessment of LV volume and ejection fraction. *J Nucl Med.* 2001;42(5):741.
34. Block S, Schaefer W, Nowak B, et al. Comparison of left ventricular ejection fraction calculated by ECG-gated PET and contrast left ventriculography. *J Nucl Med.* 2001;42(5):734.
35. Willemsen AT, Siebelink HJ, Blanksma PK, et al. Left ventricle ejection fraction determination with gated (18)FDG-PET. *J Nucl Med.* 1999;40(5):166P–166P.
36. Cooke CD, Folks RD, Oshinski JN, et al. Determination of ejection fraction and myocardial volumes from gated FDG PET studies: a preliminary validation with gated MR. *J Nucl Med.* 1997;38(5):198–198.
37. Burger C, Goerres G, Schoenes S, et al. PET attenuation coefficients from CT images: experimental evaluation of the transformation of CT into PET 511-keV attenuation coefficients. *Eur J Nucl Med Mol Imaging.* 2002;29(7):922–927.
38. Koepfli P, Wyss CA, Hany TF, et al. Evaluation of CT-transmission for attenuation correction in quantitative myocardial perfusion measurement using a combined PET-CT scanner: a pilot dose-finding study for different CT energies. *Circulation.* 2001;104(17):2778.
39. Koepfli P, Hany TF, Wyss CA, et al. CT Attenuation correction for myocardial perfusion quantification using a PET/CT hybrid scanner. *J Nucl Med.* 2004;45:537–542.
40. Kinahan PE, Hasegawa BH, Beyer T. X-ray-based attenuation correction for positron emission tomography/computed tomography scanners. *Semin Nucl Med.* 2003;33(3):166–179.
41. Nakamoto Y, Osman M, Cohade C, et al. PET/CT: comparison of quantitative tracer uptake between germanium and CT transmission attenuation-corrected images. *J Nucl Med.* 2002;43(9):1137–1143.
42. Visvikis D, Costa DC, Croasdale I, et al. CT-based attenuation correction in the calculation of semi-quantitative indices of F-18 FDG uptake in PET. *Eur J Nucl Med Mol Imaging.* 2003;30(3):344–353.
43. LeMeunier L, Maass-Moreno R, Carrasquillo JA, et al. PET/CT imaging: effect of respiratory motion on apparent myocardial uptake. *J Nucl Cardiol.* 2006;13:821–830.
44. Vass M, Sasaki K, Pan T. Investigation of heart motion with multi-slice cardiac CT for attenuation correction of PET emission data. *Radiology.* 2002;225:520–520.
45. Dizendorf E, Hany TF, Buck A, et al. Cause and magnitude of the error induced by oral CT contrast agent in CT-based attenuation correction of PET emission studies. *J Nucl Med.* 2003;44(5):732–738.
46. Nakamoto Y, Chin BB, Kraitchman DL, et al. Effects of nonionic intravenous contrast agents at PET/CT imaging: phantom and canine studies. *Radiology.* 2003;227(3):817–824.
47. Cohade C, Osman M, Nakamoto Y, et al. Initial experience with oral contrast in PET/CT: phantom and clinical studies. *J Nucl Med.* 2003;44(3):412–416.
48. Burger CN, Dizendorf EV, Hany TF, et al. Impact of transient oral contrast agent on CT-based attenuation correction in combined PET/CT studies. *Radiology.* 2002;225:409–409.
49. Antoch G, Jentzen W, Stattaus J, et al. Effect of oral contrast agents on CT-based PET attenuation correction in dual-modality PET/CT tomography. *Radiology.* 2002;225:423–424.
50. Pan T. Comparison of helical and cine acquisitions for 4D-CT imaging with multislice CT. *Med Phys.* 2005;32(2):627–634.
51. Beyer T, Antoch G, Blodgett T, et al. Dual-modality PET/CT imaging: the effect of respiratory motion on combined image quality in clinical oncology. *Eur J Nucl Med Mol Imaging.* 2003;30(4):588–596.
52. Goerres G, Buehler TC, Burger C, et al. CT based attenuation correction using a combined PET/CT scanner:

- influence of the respiration level on measured FDG concentration in normal tissues. *J Nucl Med.* 2002;43(5):887.
53. Goerres GW, Kamel E, Heidelberg TNH, *et al.* PET-CT image co-registration in the thorax: influence of respiration. *Eur J Nucl Med Mol Imaging.* 2002;29(3):351–360.
54. Goerres GW, Burger C, Kamel E, *et al.* Respiration-induced attenuation artifact at PET/CT: technical considerations. *Radiology.* 2003;226(3):906–910.
55. Osman MM, Cohade C, Nakamoto Y, *et al.* Respiratory motion artifacts on PET emission images obtained using CT attenuation correction on PET-CT. *Eur J Nucl Med Mol Imaging.* 2003;30(4):603–606.
56. Bacharach SL. PET/CT attenuation correction: breathing lessons. *J Nucl Med.* 2007;48:677–679.
57. Pan T, Mawlawi O, Nehmeh SA. Attenuation correction of PET images with respiration-averaged CT images in PET/CT. *J Nucl Med.* 2005;46:1481–1487.
58. Cook RAH, Carnes G, Lee TY, *et al.* Respiration-averaged CT for attenuation correction in canine cardiac PET/CT. *J Nucl Med.* 2007;48:811–818.